Available online at www.sciencedirect.com
SCIENCE DIRECT
Trans. Nonferrous Met. Soc. China 17(2007) 929−933
Transactions of Nonferrous Metals Society of China
www.csu.edu.cn/ysxb/

Microstructure and mechanical properties of Zr-Cu-Al bulk metallic glasses

MA Wen-jie(马文杰)[1], WANG Yu-ren(王育人)[1], WEI Bing-chen(魏炳忱)[1], SUN Yu-feng(孙玉峰)[2]

1. National Microgravity Laboratory, Institute of Mechanics, Chinese Academy of Sciences, Beijing 100080, China;
2. Research Center for Materials, Department of Materials Science and Engineering, Zhengzhou University, Zhengzhou 450002, China

Received 19 September 2006; accepted 18 June 2007

Abstract: $Zr_{49}Cu_{46}Al_5$ and $Zr_{48.5}Cu_{46.5}Al_5$ bulk metallic glasses(BMGs) with diameter of 5 mm were prepared through water-cooled copper mold casting. The phase structures of the two alloys were identified by X-ray diffractometry(XRD). The thermal stability was examined by differential scanning calorimetry(DSC). $Zr_{49}Cu_{46}Al_5$ alloy shows a glass transition temperature, T_g, of about 689 K, an crystallization temperature, T_x, of about 736 K. The $Zr_{48.5}Cu_{46.5}Al_5$ alloy shows no obvious exothermic peak. The microstructure of the as-cast alloys was analyzed by transmission electron microscopy(TEM). The aggregations of CuZr and $CuZr_2$ nanocrystals with grain size of about 20 nm are observed in $Zr_{49}Cu_{46}Al_5$ nanocrystalline composite, while the $Zr_{48.5}Cu_{46.5}Al_5$ alloy containing many CuZr martensite plates is crystallized seriously. Mechanical properties of bulk $Zr_{49}Cu_{46}Al_5$ nanocrystalline composite and $Zr_{48.5}Cu_{46.5}Al_5$ alloy measured by compression tests at room temperature show that the work hardening ability of $Zr_{48.5}Cu_{46.5}Al_5$ alloy is larger than that of $Zr_{49}Cu_{46}Al_5$ alloy.

Key words: bulk metallic glass; mechanical properties; nanocrystalline composite

1 Introduction

In recent years, bulk metallic glasses(BMGs) have attracted broad attention due to their importance in both theoretical study and industrial applications[1−2]. As a very promising structure material, BMGs have unique properties such as high yield strength, high hardness, and excellent corrosion and wear resistance[3]. However, the high strength of BMGs is often accompanied by remarkably decrease of plastic deformation, which greatly limits their application as engineering materials [4]. Based on this reason, BMG based composites are well developed to improve the plastic deformation ability of the BMGs[5]. For example, it has been found that addition of Pd, Pt, Au in ternary Zr-Cu-Al metallic glasses can induce the formation of nanostructure composed of Zr_2(Cu, M) (M=Pd, Pt or Au) and remain amorphous phase during annealing. These nanocrystalline alloys show better bending ductility and higher tensile fracture strength than the corresponding Zr-based monolithic amorphous alloys[6]. Zr-Ti-Cu-Ni-Be system has large glass forming ability, which has drawn plenty of intensive investigations because of its excellent properties, including high strength and high hardness[7]. HAYS et al[8] developed a Zr-Ti-Cu-Ni-Be BMG composite containing BCC dectile dendritic β solid solution as toughening phase by adding Nb to the alloy melt. The composite exhibits remarkably improved plastic deformation and obvious strain hardening on the premise of preserving its high fracture strength. Besides, SUN et al[9] reported that $Zr_{48.5}Cu_{46.5}Al_5$ bulk metallic glass matrix composites with diameters of 3 mm and 4 mm formed a microstructure with coexistence of CuZr martensite plate and nanocrystalline Zr_2Cu and $Cu_{10}Zr_7$. Room temperature compression tests reveal that these composites exhibit obvious strain hardening and plastic deformation prior to failure. JAYANTA et al[10] suggested that the work hardening capability and ductility of Cu-Zr-Al metallic glass are attributed to an unique structure correlated with atomic-scale inhomogeneity, which leads to extensive shear band formation, interactions, and multiplication of shear bands. Work hardening is an interesting question, because

Foundation item: Project(KJCX2-SW-L05) supported by the Knowledge Innovation Program of Chinese Academy of Sciences
Corresponding author: WANG Yu-ren; Tel: +86-10-62614945; E-mail: wangyr@imech.ac.cn

BMGs usually do not show strain hardening during deformation as ductile metals do, but exhibit strain softening and thermal softening instead[11]. In order to further clarify the microstructure—property relationship, we produced $Zr_{49}Cu_{46}Al_5$ alloy containing nanocrystals and $Zr_{48.5}Cu_{46.5}Al_5$ alloy containing CuZr martensite plates. The effect of the size and distribution of CuZr crystalline phase on the deformation behavior was studied.

2 Experimental

$Zr_{49}Cu_{46}Al_5$ and $Zr_{48.5}Cu_{46.5}Al_5$ alloys were prepared by arc melting under a Ti-gettered argon atmosphere. Bulk glassy alloy rods in a cylindrical shape with a length of 80 mm and diameter of 5 mm were prepared by the copper mold casting method. The resulting samples were cut, polished, etched, and then observed by optical microscopy(OM). The phase structures of all samples were identified by X-ray diffractometry. The microstructure and fracture morphology of the as-cast alloys were analyzed by transmission electron microscopy(TEM) and scanning electron microscopy (SEM). To produce TEM specimen, disks with a thickness of about 0.5 mm were cut from the rods. Samples for TEM analysis were prepared first by mechanical grinding to be about 50 μm in thickness and finally thinned by ion milling. The thermal stability was examined by differential scanning calorimetry(DSC) with a heating rate of 20 K/min. Cylindrical specimens of 5 mm in diameter and 10 mm in length were prepared from the as-cast rods, and tested in an MTS testing machine under quasistatic loading (initial stain rate of 1×10^{-4} s^{-1}) at room temperature.

3 Results and discussion

Fig.1 shows the X-ray diffraction patterns of the alloys. For $Zr_{48.5}Cu_{46.5}Al_5$ alloy, apart from CuZr phase that is monoclinic with lattice parameters of a=0.330 1 nm, b=0.413 8 nm, c=0.527 3 nm, and β=104.7°, few diffraction peaks identified as $Cu_{10}Zr_7$ are also found. For $Zr_{49}Cu_{46}Al_5$ alloy, two small crystalline diffraction peaks superimposed on the broad amorphous diffraction peak are identified as CuZr phase, which has a cubic structure, with the lattice constant of a=0.325 6 nm.

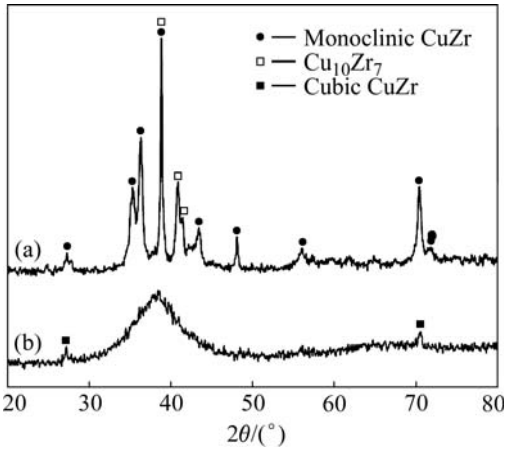

Fig.1 X-ray diffraction patterns of alloys: (a) $Zr_{48.5}Cu_{46.5}Al_5$; (b) $Zr_{49}Cu_{46}Al_5$

DSC curves of $Zr_{49}Cu_{46}Al_5$ and $Zr_{48.5}Cu_{46.5}Al_5$ alloy rods are shown in Fig.2. $Zr_{49}Cu_{46}Al_5$ alloy shows a glass transition temperature, T_g, of about 689 K, an crystallization temperature, T_x, of about 736 K and a supercooled liquid interval, ΔT_x ($=T_x-T_g$), of 47 K. $Zr_{48.5}Cu_{46.5}Al_5$ alloy shows no obvious exothermic peak, which indicates the much less amount of amorphous phase.

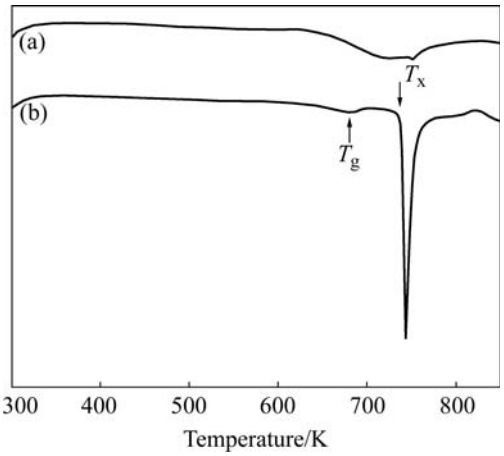

Fig.2 DSC curves of $Zr_{48.5}Cu_{46.5}Al_5$ (a) and $Zr_{49}Cu_{46}Al_5$ (b) alloys

Fig.3 shows optical micrographs of $Zr_{49}Cu_{46}Al_5$ and $Zr_{48.5}Cu_{46.5}Al_5$ alloys. Some spherical-like islands distribute non-uniformly in the amorphous matrix of $Zr_{49}Cu_{46}Al_5$ alloy, while large areas of crystalline regions are found on the surface of $Zr_{48.5}Cu_{46.5}Al_5$ alloy. According to the results of optical micrographs, it is found that although the compositions of two alloys are very close, the microstructures are quite different.

Fig.4(a) shows the bright-field TEM image of $Zr_{49}Cu_{46}Al_5$ alloy and the corresponding selected-area diffraction pattern. It is seen that nanocrystals are embedded in the amorphous matrix and distribute randomly. The particles can be identified to be a mixture of nanocrystalline CuZr and $CuZr_2$ according to the SAED pattern. In addition, an interesting phenomenon is found that some nanocrystals connect together. Fig.4(b) shows HRTEM image of $Zr_{49}Cu_{46}Al_5$ alloy. Clearly, the morphology is composed of aggregations of nanosized crystallites. Nanocrystal has a size of about 20 nm. The lattice image is randomly oriented in each region and hence each nanocrystal appears with a random orienta-

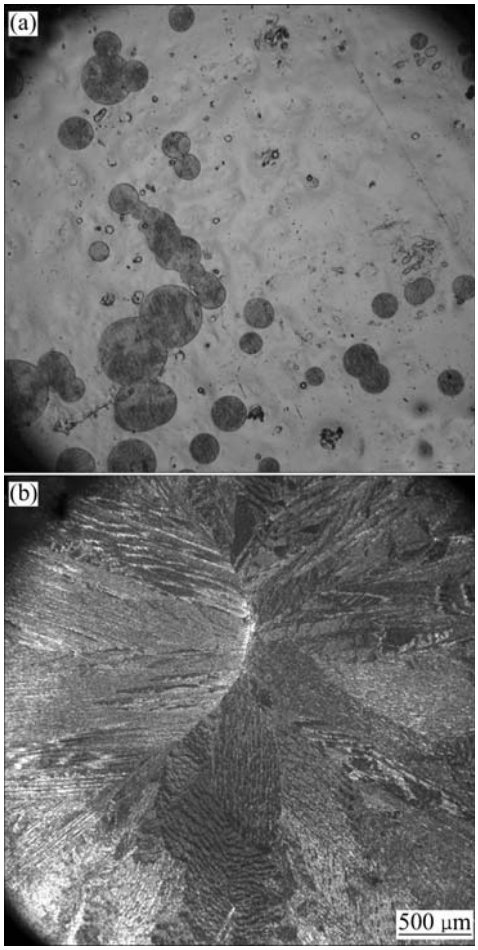

Fig.3 Optical micrographs of alloys: (a) $Zr_{49}Cu_{46}Al_5$; (b) $Zr_{48.5}$-$Cu_{46.5}Al_5$

tion. The microstructure is quite different from that of $Zr_{48.5}Cu_{46.5}Al_5$ alloy. The bright-field TEM image of $Zr_{48.5}Cu_{46.5}Al_5$ alloy is shown in Fig.4(c). It can be seen that CuZr plates consist of a large amount of stacking faults. The CuZr phase is thought to be a martensite phase. The XRD result (Fig.1(a)) indicates that CuZr phase is a monoclinic structure, which is consistent with the microstructure of the martensite phase in CuZr compound, as pointed out in previous studies[12−15].

The stress—stain curves of $Zr_{49}Cu_{46}Al_5$ and $Zr_{48.5}Cu_{46.5}Al_5$ alloys are shown in Fig.5. According to the curves shown in Fig.5, $Zr_{49}Cu_{46}Al_5$ alloy exhibits a yield strength of 1 554 MPa, an ultimate compressive strength of 2 037 MPa, and plastic strain of 6.0%. For $Zr_{48.5}Cu_{46.5}Al_5$ alloy, the ultimate fracture strength (σ_f= 1 607 MPa) is obviously lower than that of $Zr_{49}Cu_{46}Al_5$ alloy. According to Ref.[16], crystalline specimens of the same nominal composition show significantly lower values of fracture strength. The room temperature compression results are in good agreement with the report. In addition, $Zr_{48.5}Cu_{46.5}Al_5$ alloy shows a yield strength of about 310 MPa. The yield point of it is not

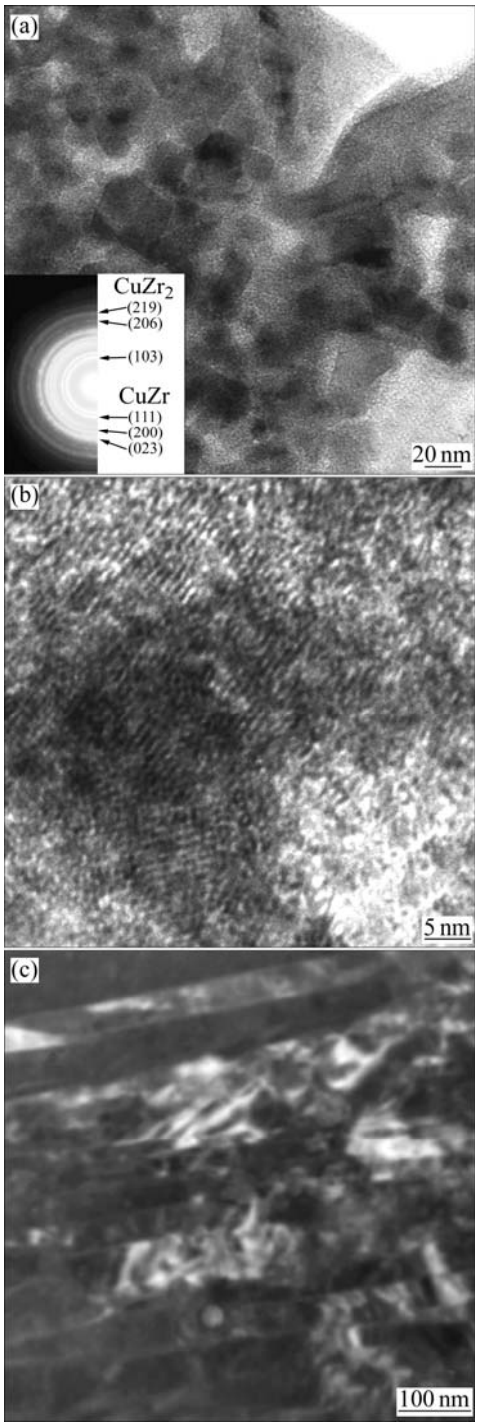

Fig.4 TEM images of $Zr_{49}Cu_{46}Al_5$ and $Zr_{48.5}Cu_{46.5}Al_5$ alloy: (a) Nanocrystals embedded in amorphous matrix in $Zr_{49}Cu_{46}Al_5$ alloy; (b) HRTEM image showing aggregation of nanocrystals in $Zr_{49}Cu_{46}Al_5$ alloy; (c) CuZr martensite plates in $Zr_{48.5}Cu_{46.5}Al_5$ alloy

obvious, and the original elastic modulus is about 53 GPa. Although the stress—strain curves from both BMGs clearly reveal a stress increase with further increasing strain, the slope change of the stress—strain curves after yielding is much larger for $Zr_{48.5}Cu_{46.5}Al_5$

alloy than for $Zr_{49}Cu_{46}Al_5$ alloy. This means that the former exhibits a significant strain-hardening feature due to the presence of amount of martensite phases.

Fig.6 shows the fracture morphologies of two alloys. For $Zr_{49}Cu_{46}Al_5$ alloy, the compressive fracture takes place along the maximum shear plane that is declined by about 45° to the direction of compressive load. The fracture morphology of $Zr_{49}Cu_{46}Al_5$ nanocrystalline alloy is shown in Fig.6(a), which has a typical characteristic of ductile fracture with well-developed vein pattern. Furthermore, Fig.6(b) shows that the shear bands are highly branched on some regions of the same specimen surface. The shear band spacing is estimated to be 500−800 nm. The SEM image of the whole fractured surface of $Zr_{48.5}Cu_{46.5}Al_5$ alloy is shown in Fig.6(c). The fractured surface consists of many steep slipped planes and secondary fractured crevices. In addition, some molten droplets can be found on the fracture surface of $Zr_{48.5}Cu_{46.5}Al_5$ alloy (Fig.6(d)).

The above results show that microstructure and deformation behavior of Zr-Cu-Al system alloys are quite sensitive to the chemical composition. The aggregations of the nanocrystals in $Zr_{49}Cu_{46}Al_5$ alloy hinder the propagation of the shear bands; and enable their branching to lead to global ductility. When the nanocrystals are very small and separated by the amorphous matrix, they can not block the propagation of the shear bands[17]. When the nanocrystals occupy large volumetric fraction and the crystals are connected, they will act as an obstacle to the local shear deformation, thus retarding the shear fracture of the alloy[18]. Therefore, the $Zr_{49}Cu_{46}Al_5$ alloy exhibits high strength and large plastic strain at the same time. Compared with the elastic-perfect plastic deformation feature during

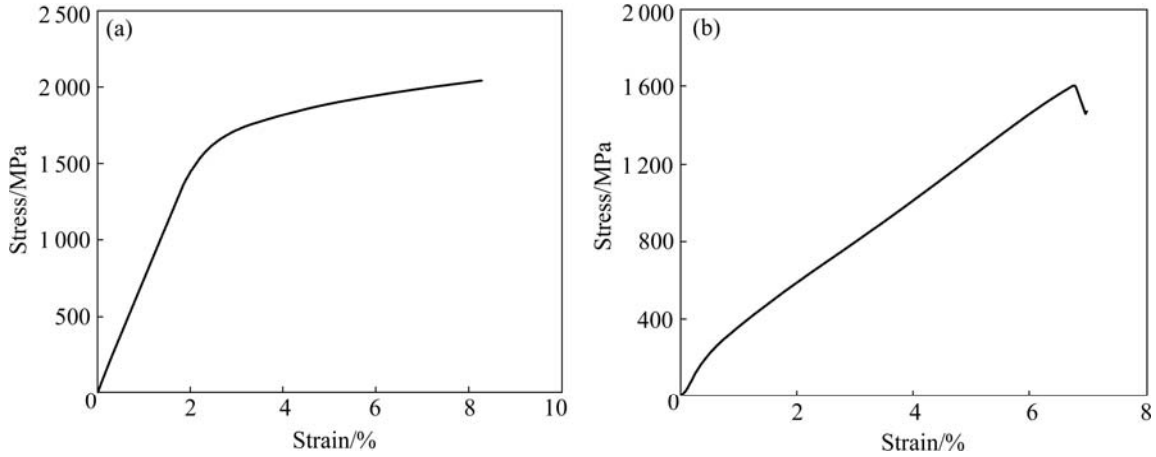

Fig.5 Compressive strain—stress curves: (a) $Zr_{49}Cu_{46}Al_5$ alloy; (b) $Zr_{48.5}Cu_{46.5}Al_5$ alloy

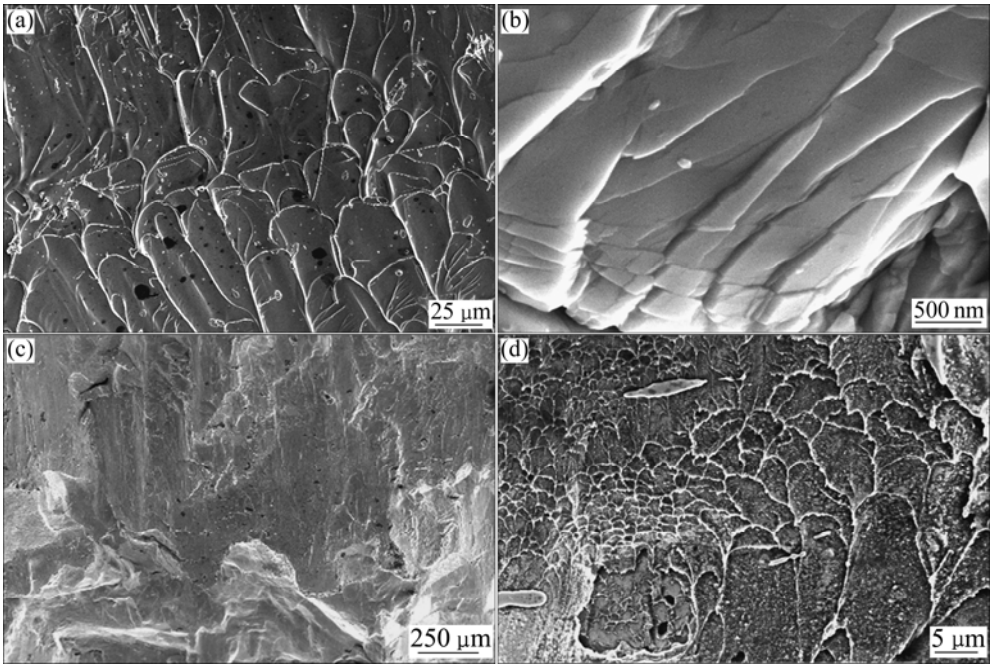

Fig.6 Fracture morphologies of $Zr_{49}Cu_{46}Al_5$ and $Zr_{48.5}Cu_{46.5}Al_5$: (a) Well-developed vein patterns of $Zr_{49}Cu_{46}Al_5$ alloy; (b) Shear band of $Zr_{49}Cu_{46}Al_5$ alloy; (c) and (d) Fractured surface of $Zr_{48.5}Cu_{46.5}Al_5$ alloy

compressive test, $Zr_{48.5}Cu_{46.5}Al_5$ alloy containing large amount of martensite plates exhibits a significant strain hardening without distinct yielding phenomenon. This significant strain hardening is caused by the presence of many CuZr martensite plates. It is suggested that the size and distribution of CuZr martensite plate have significant influence on the deformation behavior of the alloys. $Zr_{49}Cu_{46}Al_5$ alloy in this study may also contain a small amount of martensite plate, but the volume fraction is too small to be identified by XRD. Compared with previous reports, the strain hardening ability of the present $Zr_{48.5}Cu_{46.5}Al_5$ alloy with diameter of 5 mm is also larger than that of $Zr_{48.5}Cu_{46.5}Al_5$ alloy with diameter of 3 mm or 4 mm[8]. The reason may be that for $Zr_{48.5}Cu_{46.5}Al_5$ alloy with diameter of 5 mm, CuZr martensite phase distributes in whole region of the sample, while for $Zr_{48.5}Cu_{46.5}Al_5$ with diameter of 3 mm and 4 mm, the micrometer sized CuZr martensite phase distributes in the central region of the sample. The difference of volume fraction and distribution of martensite plate results in the difference of deformation behavior. Therefore, it is suggested that the plastic deformation behavior, especially the strain hardening feature, is sensitive to the size and distribution of nanocrystals or martensite phases.

According to Ref.[19], the metallographic method of pinpointing the best glass forming alloy has been used in Zr-Cu-Al alloy. They have pinpointed the three best glass forming regions, $Zr_{48}Cu_{45}Al_7$, $Zr_{45}Cu_{49}Al_6$, and $Zr_{54}Cu_{38}Al_8$ and $Zr_{56}Cu_{36}Al_8$ in three adjacent eutectics. The best glass formers were surrounded by the alloys forming crystalline and amorphous composite with similar size. Therefore, it is worth noting that near the composition of $Zr_{48}Cu_{46}Al_5$ alloy, the microstructures of the materials are rather complex. CuZr phase in the amorphous matrix can either exist in nanocrystals or transform into martensite phase, sometimes can occur a eutectoid reaction $CuZr \rightarrow Cu_{10}Zr_7+CuZr_2$ at about 988 K[20]. Tiny change of the composition will bring enormous changes in the microstructure of Zr-Cu-Al alloy, resulting in the differences of mechanical properties. By changing the composition slightly, the BMGs with more excellent mechanical property may be found.

4 Conclusions

1) The mechanical properties of Zr-Cu-Al bulk metallic glasses are sensitive to the size and distribution of CuZr crystalline phase.

2) The strain hardening ability of $Zr_{48.5}Cu_{46.5}Al_5$ alloy is larger than that of $Zr_{49}Cu_{46}Al_5$ alloy. The size and distribution of CuZr martensite plate in Zr-Cu-Al alloy have important influence on the deformation behavior.

References

[1] INOUE A, ZHANG W. Formation, thermal stability and mechanical properties of Cu-Zr-Al bulk glassy alloys [J]. Mater Trans, 2002, 43(11): 2921−2925.

[2] PEKER A, JOHNSON W L. A highly processable metallic glass: $Zr_{41.2}Ti_{13.8}Cu_{12.5}Ni_{10.0}Be_{22.5}$ [J]. Appl Phys Lett, 1993, 63: 2342−2344.

[3] INOUE A. Stabilization of metallic supercooled liquid and bulk amorphous alloys [J]. Acta Mater, 2000, 48: 279−306.

[4] CHOI-YIM H, BUSCH R, KOSTER U, JOHNSON W L. Synthesis and characterization of particulate reinforced $Zr_{57}Nb_5Al_{10}Cu_{15.4}Ni_{12.6}$ bulk metallic glass composites [J]. Acta Mater, 1999, 47: 2455−2462.

[5] CHOI-YIM H, JOHNSON W L. Bulk metallic glass matrix composites [J]. Appl Phys Lett, 1997, 71: 3808−3891.

[6] HAYS C C, KIM C P, JOHNSON W L. Improved mechanical behavior of bulk metallic glasses containing in situ formed ductile phase dendrite dispersion [J]. Mater Sci Eng A, 2001, 304/306: 650−655.

[7] ZHANG Ke-qin, LU Qi-zhu. Deformation of $Zr_{41}Ti_{14}Cu_{12.5}Ni_{10}Be_{22.5}$ bulk amorphous alloy under isobaric pressure in super-cooled liquid region [J]. Trans Nonferrous Met Soc China, 2005, 15: 612−614.

[8] HAYS C C, KIM C P, JOHNSON W L. Microstructure controlled shear bands pattern formation and enhanced plasticity of bulk metallic glasses containing in situ formed ductile phase dendrite dispersion [J]. Phys Rev Lett, 2000, 80: 2478−2490.

[9] SUN Yu-feng, WEI Bing-chen, WANG Yu-ren, LI Wei-huo, CHWUNG T L, SHEK C H. Plasticity-improved Zr-Cu-Al bulk metallic glass matrix composites containing martensite phase [J]. Appl Phys Lett, 2005, 87: 051905.

[10] JAYANTA D, TANG Mei-bo, KIM K B, RALF T, FALKO B, WANG Wei-hua, Jurgen E. "Work-Hardenable" ductile bulk metallic glass [J]. Phys Rev Lett, 2005, 94: 205501.

[11] SCHOERS J, WILLIAM L, JOHNSON W L. Ductile bulk metallic glass [J]. Phys Rev Lett, 1994, 93: 255506.

[12] NICHOLLS A, HARRIS W. Indentification of phase resulting from the transformation of the intermetallic phase ZrCu [J]. J Mater Sci Lett, 1986, 5: 217−220.

[13] CARVALHO E, HARRIS M. Constitutional and structural studies of the intermetallic phase, ZrCu [J]. J Mater Sci Lett, 1980, 15: 1224−1230.

[14] SEO J W, SCHRYVER D. TEM investigation of the microstructure and defects of CuZr martensite (I): Morphology and twin systems [J]. Acta Mater, 1998, 46: 1165−1175.

[15] SEO J W, SCHRYVER D. TEM investigation of the microstructure and defects of CuZr martensite (II): Planar defects [J]. Acta Mater, 1998, 46: 1177−1183.

[16] FAN C, INOUE A. Ductility of bulk nanocrystalline composites and metallic glasses at room temperature [J]. Appl Phys Lett, 2000, 77(1): 46−48.

[17] XING L Q, BERTRAND C, DALLAS J P, CORNET M. Nanocrystal evolution in bulk amorphous $Zr_{57}Cu_{20}Al_{10}Ni_8Ti_5$ alloy and its mechanical properties [J]. Mater Sci Eng A, 1998, 241: 216−225.

[18] BIAN Z, CHEN G L, HE G, HUI X D. Microstructure and ductile-brittle transition of as-cast Zr-based bulk glass alloys under compressive testing [J]. Mater Sci Eng A, 2001, 316: 135−144.

[19] WANG D, TAN H, LI Y. Multiple maxima of GFA in three adjacent eutectics in the Zr-Cu-Al alloy system—A metallographic way to pinpoint the best glass forming alloys [J]. Acta Mater, 2005, 53: 2969−2979.

[20] LIU Z Y, AINDOW M, HRIJAC J A, HARRIS I R. Phase transformations in equiatomic ZrCu alloy [J]. Mater Sci Forum, 2001, 360/362: 223−228.

(Edited by YANG Bing)